JOURNAL OF Materials CHEMISTRY

# Microemulsion synthesis and electrocatalytic properties of platinum–cobalt nanoparticles

**Xin Zhang**[a,b] **and Kwong-Yu Chan***[b]

[a]*Department of Chemistry, Shantou University, Shantou, China 515063*
[b]*Department of Chemistry, The University of Hong Kong, Pokfulam Road Hong Kong SAR, China. Fax: (852) 28571586; E-mail: hrsccky@hku.hk*

***Received 10th October 2001, Accepted 16th January 2002***
***First published as an Advance Article on the web 19th February 2002***

Mixed platinum–cobalt nanoparticles were prepared using a water-in-oil reverse microemulsion of water–Triton X-100–propan-2-ol–cyclohexane. Nanoparticles formed in the microemulsions were characterized by transmission electron microscopy (TEM), X-ray diffraction (XRD), and energy dispersive X-ray analysis (EDX). TEM shows the Pt–Co nanoparticles to have a narrow size distribution with an average of 3–4 nm. A uniform phase of platinum and cobalt in the nanoparticles was indicated by XRD analysis. The nanoparticles were supported on a carbon electrode with high dispersion. Even at a low precious metal loading, a high catalytic activity was demonstrated for methanol oxidation at room temperature.

## Introduction

The methodologies of nanoparticle preparation have received considerable attention in recent decades as nanoparticles possess unique and unusual physical and chemical properties.[1,2] Nano-sized materials have promising applications in many areas such as microelectronic devices,[3,4] photocatalysis,[5] electrocatalysis,[6,7] biomedical engineering[8,9] and chemical processes.[10,11] A number of techniques have been used for producing nanoparticles which include gas evaporation,[12] sol–gel methods,[13] sputtering,[14] and co-precipitation.[15] It is well documented in the scientific and patent literature that combining a transition metal element with platinum gives enhanced catalytic activities for reactions such as oxygen reduction in fuel cells and direct oxidation of methanol.[16–18] Pt–Co alloys and their compounds have been applied as oxygen-reduction catalysts and magnetic materials. They have been synthesized by techniques such as chemical reduction,[18] hydrolysis,[19] vacuum deposition,[20] and electrodeposition.[21] It is, however, difficult to control the size and size distribution, and gain a consistent nanoscopic chemical composition with these preparation techniques. With the promise of a better control of particle size, shape, size distribution, and chemical composition, the preparation of nanoparticles with water-in-oil (w/o) microemulsion has attracted increasing attention but systematic investigation is warranted.[22] The preparation of Pt–Co nanoparticles by microemulsion techniques has so far not been reported.

In this paper, we report the synthesis of Pt–Co nanoparticles using w/o microemulsions, their characterization and catalytic properties. Results of X-ray diffraction (XRD), transmission electron microscopy (TEM), energy dispersion X-ray analysis (EDX), and electrocatalysis for methanol oxidation are presented and discussed.

## Experimental

A non-ionic surfactant Triton X-100 (*t*-octylphenoxypolyethoxyethanol) from Sigma Chemical Co. was used as received. Hydrazine hydrate (99% pure), propan-2-ol and cyclohexane ($C_6H_{12}$) were from BDH Chemical Ltd. Dihydrogen hexachloroplatinate(IV) hydrate($H_2PtCl_6{\cdot}xH_2O$) was from Chempure Ltd. The cobalt source was cobaltous chloride ($CoCl_2$) from BDH Chemicals Ltd. Deionized (18.2 MΩ) water produced by a Milli-Q ultrapure water unit from Millipore Ltd. was used to prepare all the aqueous solutions. Preparation of the Pt–Co nanoparticles was a two-emulsion technique as described for making other nanoparticles.[23–25] The microemulsion system used in this study consisted of Triton X-100 as a surfactant, propan-2-ol as a co-surfactant, cyclohexane as the continuous oil phase, and the Pt–Co aqueous solution or hydrazine aqueous solution as the dispersed aqueous phase. The two microemulsions had identical fractions except for the aqueous phase compositions, as indicated in Table 1. The aqueous phase in microemulsion II contains the hydrazine solution as the reducing agent and is in slight stoichiometric excess as compared with an equal amount of Pt–Co containing aqueous phase, microemulsion I. Each microemulsion system was prepared separately by mixing (by volume) 10% surfactant, 35% cyclohexane, 40% propan-2-ol and 15% aqueous phase. The microemulsion thus prepared was cloudy. A small amount of additional propan-2-ol was then titrated slowly into the microemulsion system with stirring until the microemulsion system became transparent, this indicated a size reduction of the microemulsions. The colour of the microemulsion system was between yellow and pink, reflecting the colour of the $PtCl_6^{2-}$ and $Co^{2+}$ ions. Then the two types of stable microemulsions were mixed and stirred with a stirrer. Pt–Co nanoparticles were formed by contact between a droplet of $H_2PtCl_6-CoCl_2$ containing solution and a droplet of reducing solution when they were mixed in the presence of the oil phase. The transparent solution turned black/gray due to the suspended reduced metal nanoparticles. Pure Pt nanoparticles

**Table 1** Compositions of the microemulsion systems used for the synthesis of the Pt–Co nanoparticles

| | Microemulsion I | Microemulsion II | Volume/ml (vol%) |
|---|---|---|---|
| Aqueous phase | 40 mM $H_2PtCl_6$ + 120 mM $CoCl_2$ | 0.3 M Hydrazine | 1.5 (15) |
| Surfactant | Triton X-100 | Triton X-100 | 1 (10) |
| Co-surfactant | Propan-2-ol | Propan-2-ol | 4 (40) |
| Oil phase | Cyclohexane | Cyclohexane | 3.5 (35) |

DOI: 10.1039/b109223e

were prepared by the same method but with only $H_2PtCl_6$ in the aqueous phase, as indicated in Table 2.

The size and shape of the nanoparticles prepared were characterized with a TEM (JEOL 2000FX, Japan). The TEM sample was prepared by placing a 100 μl droplet of microemulsion containing the Pt–Co (reduced) nanoparticles onto a carbon TEM grid and allowing it to dry in a dry box at room temperature. Elemental analysis was obtained by a scanning EM (Cambridge S360 UK) with EDX detector (Oxford Link pertafet). The XRD measurements were performed on a (Siemens, D-5000) X-ray diffractometer using Cu-Kα radiation ($\lambda = 0.1542$ nm). The sample for XRD analysis was made of carbon Vulcan 72 powder added into the microemulsions to adsorb the Pt–Co nanoparticles and then heated at 400 °C in a nitrogen atmosphere. Without adding carbon powder, the microemulsions containing the nanoparticles remained suspended giving a black–gray appearance for many weeks. The adsorption of the microemulsion and nanoparticles by the carbon was apparent as the carbon gradually settled over a few days to leave a colorless transparent liquid above. Centrifugation can accelerate the separation of the nanoparticles and carbon from solution. The settled or centrifuged carbon was analyzed and found to contain high concentration of the metals.

The two microemulsion systems described in Table 1 were thoroughly mixed to achieve a reduction to Pt–Co particles. A circular carbon paper electrode with a 9 mm diameter (area 0.64 $cm^2$) was used as the substrate for the Pt–Co nanoparticle electrocatalysis studies. For the electrode preparation, a suspension of 0.87 mg Pt $ml^{-1}$ microemulsion was pipetted onto the surface of the carbon paper electrode. The carbon paper electrode used was an ELAT as supplied by E-TEK Inc., MA, USA. The platinum loading was calculated by the amount of solution added onto the known surface area of the carbon electrode, assuming a complete and uniform adsorption. As indicated above for the adsorption by Vulcan 72 carbon powder, the adsorption of nanoparticles was easy. After evaporation of the solvent in a dry box, the carbon electrode was immersed several times in ethanol and then dried in air. When immersed into an aqueous electrolyte solution, the electrodes thus prepared did not have nanoparticles redissolved and the electrolyte solution remained clear throughout. The Pt–Co nanoparticle/carbon electrode and the pure Pt nanoparticle/carbon electrode had the same noble metal loading of 0.5 mg $cm^{-2}$. For the TEM analysis, the carbon loaded with the Pt–Co nanoparticles was carefully stripped from the carbon paper and dissolved in ethanol. All electrochemical measurements were made in a three-compartment electrochemical cell. The potentiostat and galvanostat used were a Voltalab 40 from Radiometer and a BAS LG-50 from Bioanalytical Systems Inc. A Hg/HgO electrode from Kowslow Co. was used as the reference electrode for the methanol oxidation experiments in alkaline solution.

## Results and discussion

Fig. 1(a) shows a typical TEM image of Pt–Co nanoparticles prepared using w/o microemulsions. About 0.100 ml of the Pt–Co containing w/o microemulsion was dropped directly onto the TEM sample grid. The particles were spherical with diameters in the range of 3–4 nm with a narrow size distribution. Fig. 1(b) shows the sharp electron diffraction bright rings obtained from a selected area of Fig. 1(a). As opposed to a pattern of bright spots, the sharp diffraction rings indicated that nanoparticles of Pt–Co alloys are weakly crystalline, which is in agreement with the XRD results.[26] Fig. 2 is a TEM micrograph of Pt–Co nanoparticles adsorbed onto high surface area Vulcan 72 carbon; a homogeneous dispersion of Pt–Co nanoparticles is shown. The XRD results of the carbon supported Pt–Co mixture are displayed in Fig. 3(b) for $2\theta$ angles from 10° to 90°. Fig. 3(c) shows the typical pure platinum $2\theta$ peaks. Fig. 3(a) shows three characteristic peaks that are assigned to the β-Co metal structure from

**Table 2** Compositions of the microemulsion systems used for the synthesis of pure Pt nanoparticles

| | Microemulsion I | Microemulsion II | Volume/ml (vol%) |
|---|---|---|---|
| Aqueous phase | 40 mM $H_2PtCl_6$ | 0.3 M Hydrazine | 1.5 (15) |
| Surfactant | Triton X-100 | Triton X-100 | 1 (10) |
| Co-surfactant | Propan-2-ol | Propan-2-ol | 4 (40) |
| Oil phase | Cyclohexane | Cyclohexane | 3.5 (35) |

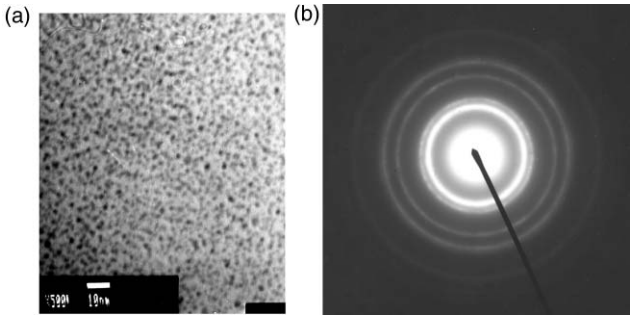


**Fig. 1** (a) TEM of Pt–Co nanoparticles prepared by microemulsion. (b) A typical electron diffraction pattern of selected areas on the same sample.

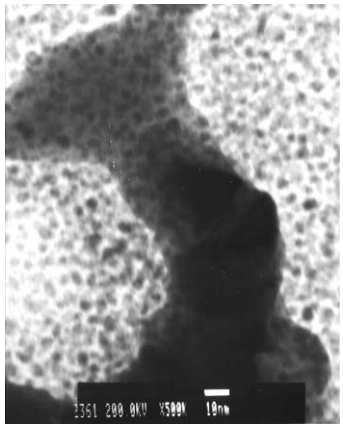

**Fig. 2** Bright-field TEM of the Pt–Co nanoparticles supported on Vulcan carbon 72.

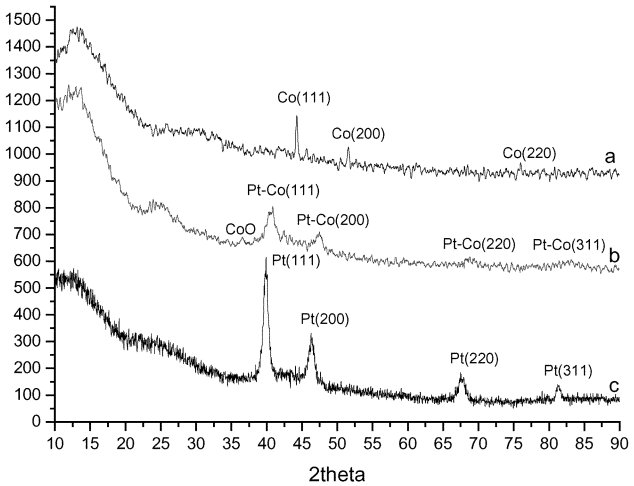


**Fig. 3** X-ray diffraction pattern of Pt–Co nanoparticles: (a) pure Co, (b) Pt–Co, (c) pure Pt.

the diffraction lines of the <111>, <200> and <220> planes. The diffraction peak positions of the Pt–Co nanoparticle mixture in Fig. 3(b) shifted to higher $2\theta$ values with respect to the characteristic peaks of pure Pt. The shift in $2\theta$ corresponds to a decreased lattice constant for platinum due to the incorporation of a Co atom. From the literature, the <111> peaks of pure Pt and pure Co are at $2\theta$ of 39.7° and 44.8°, respectively. Similar values are shown in Fig. 3(c) and Fig. 3(a). For the Pt–Co mixture, the 1 : 2.2 atom ratio translates to 68.8 atom% Co. The shift in $2\theta$ would be proportional to the atomic percentage of platinum and cobalt according to the Vegard law,[27,28] giving a theoretical value of 43.2° for the Pt–Co mixture. The $2\theta$ peak for the <111> lattice in the Pt–Co mixture of Fig. 3(b) is around 41.5°. The Vegard law may not hold with high accuracy. Alternatively, the discrepancy could be due to the existence of unalloyed Co or cobalt oxide, leading to a lower percentage of Co in the Pt–Co nanoparticle. The discrepancy could also be caused by the weak crystallinity of the Pt–Co nanoparticle alloy, which is apparent from the XRD results. The crystallinity of the Co and Pt–Co alloy phases was lower than that of the Pt phase and led to weaker intensities for the Co and Pt–Co XRD peaks. A small peak at $2\theta = 36.5°$ is associated with the cobalt oxide peak. The appearance of a separate cobalt oxide peak could be due to the coexistence of unalloyed cobalt, which as a nanoparticle in ambient air could easily form surface oxide. The EDX measurement was conducted by focusing the electron beam on several selected regions of each sample (each region of area 1 μm × 1 μm). The average composition of the samples reported gave an atom ratio of Pt : Co of 1 : 2.2. The fractional amount of Pt and Co in the different regions was in close agreement and no significant deviation from different regions was observed.

The characterization results demonstrate the possibility of preparing uniform mixed-metal nanoparticles with the reverse microemulsion technique. Control of size, composition, loading and improvement in size distribution can be made with optimization of the preparation parameters. The size of the metallic nanoparticles can be changed by using different concentrations of metal ions in the aqueous phase. Alternatively, using a non-ionic surfactant with different chain lengths or using different solvents can give different sizes of reverse microemulsions. The composition of the metal mixture in the nanoparticles can be controlled by simply varying the starting concentrations of metal ions in the aqueous phase. As the EDX results indicated, good uniformity can be achieved in the composition of the nanoparticles. This uniformity is due to good mixing and complete solubility of the metal ions in the aqueous phase. The preparation of mixed-metal particles by the microemulsion technique therefore holds good promise for other types of binary or ternary mixtures of metals for fuel cell applications.

During mixing of the two types of microemulsions, larger nanoparticles will be formed if contact between two Pt–Co containing microemulsions occurred before their individual contacts with the microemulsion containing the reducing agent. This can be minimized by using a more dilute (low number density) Pt–Co microemulsion system prepared by a smaller fraction of the aqueous phase of the first microemulsion system and a higher fraction of the hydrazine phase in the second microemulsion system. A higher Pt–Co concentration and a more dilute hydrazine concentration in the corresponding aqueous phases will keep the same stoichiometry. Further experiments are needed to verify these possibilities.

The Pt : Co ratio and the dispersion on the carbon are the two key factors for high catalytic activity and they are very much dependent on the preparation methods. To compare the performance of Pt–Co and Pt nanoparticles prepared by microemulsion preparation methods, we tested the catalytic activity of the Pt–Co and pure Pt nanoparticles towards

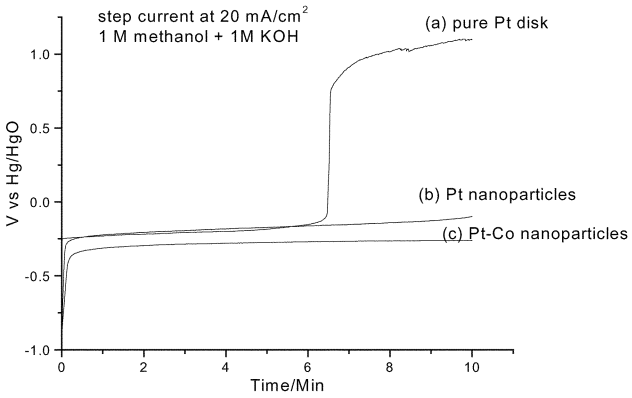


**Fig. 4** Chronopotentiograms of methanol oxidation at 20 mA cm$^{-2}$ in an equal volume mixture of 1 M methanol and 1 M KOH on: (a) pure Pt disk, (b) Pt nanoparticles/carbon, (c) Pt–Co nanoparticles/carbon.

methanol oxidation in alkaline electrolyte. The solution is prepared by mixing equal volumes of 1 M methanol solution and 1 M KOH solution. The nanoparticles were supported on a carbon paper. Fig. 4 shows the step current (chronopotentiometry) results for the room temperature oxidation of methanol by the Pt–Co nanoparticles and Pt nanoparticles on the carbon paper electrode prepared by microemulsion with the same Pt loading. With a low loading of Pt, the microemulsion prepared Pt nanoparticles gave the same activity as the pure Pt disk, but with much longer stability. The Pt disk electrode lost its catalytic ability after 6 min, probably due to carbon monoxide poisoning. This may suggest less CO adsorption by Pt nanoparticles. With the same amount of Pt, the Pt–Co nanoparticles showed better oxidation kinetics with a 50–80 mV lower oxidation potential. The optimum ratio of Pt : Co for methanol oxidation can be explored in a similar manner to the study of Pt : Co ratio in formic acid oxidation.[21]

Fig. 4 shows the time dependent polarization at only one current density. The complete polarization curve is shown in Fig. 5 (bottom axis labels) for methanol oxidation on the pure Pt and Pt–Co nanoparticles supported on carbon. A set of constant potential experiments were performed. The steady-state current was measured at 5 min after stepping the potential. The results in Fig. 5 again show the better catalytic performance of the Pt–Co nanoparticles, compared to pure Pt nanoparticles. The difference is more obvious at higher current densities or higher oxidation potentials. The top axis shows the

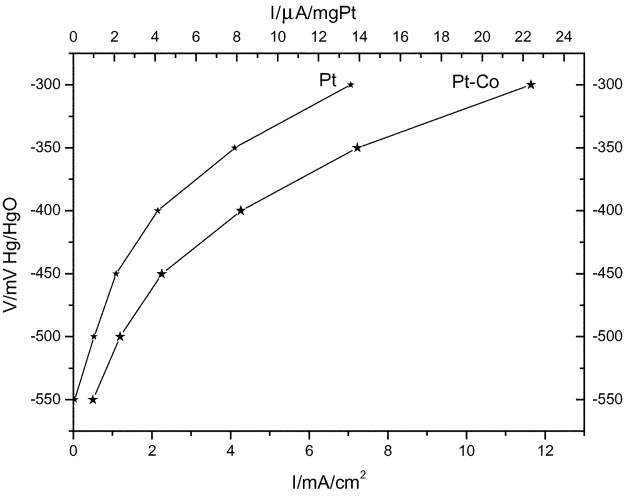


**Fig. 5** Polarization curves for oxidation of an equal volume mixture of 1 M methanol and 1 M KOH solutions at room temperature by Pt nanoparticles/carbon and Pt–Co nanoparticles/carbon. The top scale was converted to current per loading of Pt where the loading was constant at approximately 0.5 mg cm$^{-2}$.

same results of current density but plotted with respect to the noble metal loading. Alternatively, the loading effect can be studied by varying the platinum loading in different electrodes. Nonlinear behaviour may exist and more effective utilization of catalyst at a lower loading is expected. The Pt–Co/carbon paper electrode and pure Pt/carbon paper electrode both showed a good performance for the methanol oxidation. The high catalytic activity of the two electrodes could be due to particle size, uniform size distribution, and high dispersion on the carbon paper. However, the catalytic activity of the Pt–Co nanoparticle/carbon paper electrode is 1.6–2.2 times higher than that of pure Pt nanoparticle/carbon paper electrode over a wide potential range. These results demonstrate the advantage of Pt–Co binary metal nanoparticles prepared by microemulsion and their potential for fuel cell applications. The increased catalytic activity of the Pt–transition metal alloys have been studied and explained by several researchers.[16,29,30] Preparation of other mixed-metal nanoparticles, such as Pt–Ru, through the reverse microemulsion route is interesting and promising.

## Conclusions

The synthesis of Pt–Co nanoparticles through separate reverse microemulsions of water–Triton X-100–propan-2-ol–cyclohexane (w/o) has been achieved by the reduction of aqueous Pt–Co solution with hydrazine. The TEM images indicated an average size for the Pt–Co nanoparticle of 3–4 nm with a narrow size distribution. XRD results show the formation of a uniform phase of platinum and cobalt oxide and the atom ratio of Pt to Co was 1 : 2.2 from EDX analysis. The electrochemical experiments showed that the microemulsion-prepared Pt–Co nanoparticles supported on a carbon paper electrode have a higher catalytic activity toward methanol oxidation than pure Pt nanoparticles supported on a carbon paper electrode at the same Pt loading.

## Acknowledgement

This work is supported by Research Grants Council of Hong Kong (HKU 7072/019) and a HKU Foundation Seed Grant. We thank the Electron Microscope Unit and Dr J. Gao of the Physics Department for the use of TEM, EDX and XRD

## References

1 R. F. Service, *Science*, 1996, **271**, 920.
2 R. W. Siegel, *Phys. Today*, 1993, **46**(10), 64.
3 V. L. Colvin, M. C. Schlamp and A. P. Alivisatos, *Nature*, 1994, **370**, 354.
4 M. J. Sugimoto, *Am. Ceram. Soc.*, 1999, **82**, 269.
5 A. J. Hoffman, G. Mills, H. Yee and M. R. Hoffmann, *J. Phys. Chem.*, 1992, **96**, 5546.
6 L. Brus, *J. Phys. Chem.*, 1986, **90**, 2555.
7 S. H. Joo, S. J. Choi, I. Oh, J. Kwak, Z. Liu, O. Terasaki and R. Ryoo, *Nature*, 2001, **412**, 169.
8 U. Hafeli, W. Schutt, J. Teller and M. E. Zborowski, *Scientific and Clinical Applications of Magnetic Carriers*, Plenum, New York, 1997.
9 S. Santra, K. Wang, R. Tapec and W. Tan, *J. Biomed. Opt.*, 2001, **6**, 160.
10 A. Khaleel, W. F. Li and K. J. Klabunde, *Nanostruct. Mater.*, 1999, **12**, 463.
11 U. Bach, D. Lupo, P. Comte, J. E. Moser, F. Weissorted, J. Salbeck, H. Spreitzer and M. Gratzel, *Nature*, 1998, **395**, 583.
12 R. W. Siegel, *J. Mater. Rev.*, 1998, **3**, 1367.
13 B. J. Fegley, P. White and H. K. Bowen, *Am. Ceram. Soc. Bull.*, 1985, **64**, 1115.
14 P. Fayet and L. Z. Woste, *Phys. D*, 1986, **3**, 177.
15 Z. X. Jang, C. M. Sorensen, K. J. Klabunde and G. C. Hadjipanayis, *J. Colloid Interface Sci.*, 1991, **146**, 38.
16 F. J. Luczak and D. A. Landsman, *U.S. Pat.*, 4677092, 1987.
17 M. Watanabe, K. Tsurumi, T. Mizukami, T. Nakamura and P. Stonehart, *J. Electrochem. Soc.*, 1994, **141**, 2659.
18 K. Yohannes, *J. Electrochem. Soc.*, 1996, **143**, 2152.
19 M. Neergat, A. K. Shukla and S. Gandhi, *J. Appl. Electrochem.*, 2001, **31**, 373.
20 M. Thielen, S. Kirsch, A. Weinforth, A. Carl and E. F. Wassermann, *IEEE Trans. Magn.*, 1998, **34**, 1009.
21 N. Chi, K. Y. Chan and D. L. Phillips, *Catal. Lett.*, 2001, **71**, 21.
22 J. H. Fendler, *Chem. Rev.*, 1987, **87**, 877.
23 J. Wang, L. S. Ee, S. C. Ng, C. H. Chew and L. M. Gan, *Mater. Lett.*, 1997, **30**, 119.
24 M. H. Lee, C. Y. Tai and C. H. Lu, *J. Eur. Ceram. Soc.*, 1999, **19**, 2593.
25 A. S. Bommarius, J. F. Holzarth, D. I. C. Wang and T. A. Hatton, *J. Phys. Chem.*, 1990, **94**, 7232.
26 V. Kurikka, P. M. Shafi and G. Aharon, *Chem. Mater.*, 1998, **10**, 3445.
27 M. Watanabe, M. Uchida and S. Motoo, *J. Electroanal. Chem.*, 1987, **229**, 395.
28 J. Park and J. Cheon, *J. Am. Chem. Soc.*, 2001, **123**, 5743.
29 V. Jalan and E. J. Taylor, *J. Am. Chem. Soc.*, 1983, **130**, 229.
30 B. C. Beard and P. N. Ross, *J. Electrochem. Soc.*, 1988, **133**, 1839.